Solar Energy Materials and Solar Cells 173 (2017) 12–17

Contents lists available at ScienceDirect

Solar Energy Materials and Solar Cells

journal homepage: www.elsevier.com/locate/solmat

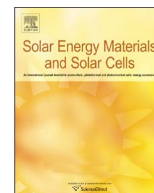

Multiple pathways for permanent deactivation of boron-oxygen defects in p-type silicon

Nitin Nampalli*, Hongzhao Li, Moonyong Kim, Bruno Stefani, Stuart Wenham, Brett Hallam, Malcolm Abbott

School of Photovoltaic and Renewable Energy Engineering, University of New South Wales, Sydney, NSW 2052, Australia

ARTICLE INFO

Keywords:
Boron-oxygen defect
Silicon
Thermal deactivation
Thermal activation
Regeneration
Hydrogen
Passivation
Carrier lifetime
Rapid thermal annealing
Belt firing

ABSTRACT

In this work, it is shown that there are at least two separate pathways for the permanent deactivation of boron-oxygen defects – a purely thermal pathway involving the dissociation of defect precursors, and another mechanism based on passivation of the fully-formed defect during an illuminated annealing process (regeneration). Based on investigations on fired and non-fired p-type Czochralski silicon wafers, a thermal reduction in the net concentration of BO defects is confirmed and found to be caused by rapid cooling following a belt-furnace firing process. This thermal deactivation occurs independently of any subsequent permanent deactivation induced by illuminated annealing and is likely related to the dissociation of the defect and subsequent loss of defect precursors to other species. Further, by varying the surface dielectric present on the wafers during a rapid thermal process, it is demonstrated that in the absence of hydrogen in the wafer bulk, applying an illuminated annealing process does not result in any significant permanent deactivation of defects. In contrast, thermal deactivation occurs independently of the presence of hydrogen in the wafer bulk. This demonstrates that permanent deactivation via the thermal pathway and that via the illuminated annealing (regeneration) pathway occur independently of each other and have different underlying mechanisms. The implications of multiple pathways for permanent deactivation are discussed and the well-known three-state model is revisited in light of this information. A fourth state to represent the end point of thermal deactivation (State D) is proposed for more accurate modelling of BO defect kinetics.

1. Introduction

The boron-oxygen (BO) defect is a well-known defect in Czochralski (Cz) silicon and is known to cause carrier-induced degradation (CID) in such material [1]. Due to its metastability, the defect exists in at least three different states [2–4]: the annealed state (State A) that is recombination inactive, the degraded state (State B) that is recombination active, and the regenerated or passivated state (State C) that is also recombination inactive. In contrast to State A, which transitions into State B upon illumination (or carrier injection), State C is relatively stable [2,3] and does not show further degradation upon carrier injection. Permanent deactivation of the defect has therefore typically been thought of as the process of transitioning the defect from State B into State C – a process typically known as regeneration, which can occur in appropriately prepared samples [5–9] by the application of an illuminated anneal process [2,3].

However, there has been considerable debate regarding the mechanism underlying the permanent deactivation process. Firstly, there is incidental evidence that the net concentration of active BO defects is dependent on the thermal history of wafers [10–12], with the cooling rate following a rapid thermal anneal (firing) suspected to have a particularly strong influence on the defect concentration [10,12]. Importantly, changes in the defect density appear to occur immediately after the thermal process and before any illuminated annealing. In addition to this, firing conditions are also known to have a strong influence on the degree of permanent deactivation achieved during subsequent illuminated annealing [5,12,13].

Some authors have proposed that all permanent deactivation of the defect occurs due to a purely thermal process wherein the defect dissociates, and the precursors are lost to other species present in the wafer [12,14,15]. While this explains, at least qualitatively, the observed kinetics of regeneration (i.e. the transition from State B to State C) as well as the influence of firing conditions on the net defect density, there is also considerable evidence that regeneration is not a purely thermal process. In particular, the presence of hydrogen in the wafer bulk has been shown to have a significant influence on the degree [5,7,9,16–18]

* Corresponding author.
E-mail address: nnampalli@gmail.com (N. Nampalli).

http://dx.doi.org/10.1016/j.solmat.2017.06.041
Received 13 April 2017; Received in revised form 19 June 2017; Accepted 19 June 2017
Available online 29 June 2017
0927-0248/ © 2017 Elsevier B.V. All rights reserved.

as well as the rate of regeneration [5,8,19]. Hence, several authors have proposed that permanent deactivation via regeneration (i.e. during illuminated annealing) occurs due to hydrogen passivation of the BO defect [7,9,20–23].

However, it is unclear if hydrogen passivation could be responsible for permanent deactivation of the defect that occurs immediately following high-temperature thermal treatments. This raises the question of whether there are in fact two independent pathways to reduce the net active BO defect density that have been conflated with one another in the literature. Further, the presence of an independent pathway suggests that for current understanding of the BO defect – the three-state model – may not be a complete description of the BO defect system.

This study aims to clarify these issues by distinguishing between the thermal reduction in active defect concentration that occurs during high-temperature processes ('thermal deactivation'), and the deactivation of fully formed defects that occurs during subsequent illuminated annealing ('regeneration'). The effects of these processes are separately quantified, and it is attempted to determine whether the mechanism underlying the two processes are related, and what role hydrogen may play in each case. Finally, the possibility of multiple independent pathways for deactivation of the BO defect is explored and its implications for the well-known three-state model for the BO defect are discussed.

2. Experimental details and methods

Symmetrical lifetime test structures were prepared using commercial grade 156 mm × 156 mm pseudo-square boron-doped Cz wafers (1.6 – 1.8 Ω cm) by alkaline texturing followed by acidic neutralisation. Wafers were subjected to an RCA clean and HF dip, then diffused at 795 °C for 25 min in a $POCl_3$ tube furnace followed by a drive-in diffusion at 885 °C for 30 min to achieve an emitter sheet resistance of 70 Ω/sq – a process known to be effective at gettering [24]. The phosphosilicate glass (PSG) and emitter thus formed were removed by etching ~2 µm from both surfaces, resulting in a wafer thickness of approximately 180 µm. This was done to ensure minimal concentrations of impurities other than B-O within the wafer bulk. The wafers were then RCA cleaned and a second, light $POCl_3$ diffusion at 780 °C for 30 min with a 20-min drive-in step was applied to achieve a sheet resistance of ~200 Ω/sq to aid in surface passivation.

The wafers were then divided into two groups and either (a) coated with silicon nitride (SiN_x:H) layers using plasma enhanced chemical vapour deposition (hydrogen-rich dielectric) at 350 °C, or (b) subjected to dry thermal oxidation at 900 °C for 6 h (hydrogen-free SiO_2 dielectric). The resulting SiN_x:H layer was 83 nm thick and had a refractive index of 2.08 at a wavelength of 633 nm [25]. The thermal oxide was 100 nm thick.

The normalised defect density (*NDD*) [26] was determined via carrier lifetime measurements performed on a Sinton Instruments WCT-120 quasi-steady-state photoconductance (QSSPC) lifetime tester. To do this, samples were annealed in the dark at 200 ± 3 °C for 10 min to obtain carrier lifetime of the samples in the 'annealed' state of the defect (τ_{DA}). Subsequently, the samples were light soaked for 48 h at 35 ± 3 °C under a halogen lamp with an intensity equivalent to 0.77 ± 0.03 suns (measured using a calibrated silicon reference cell). This was done to ensure complete degradation of carrier lifetime due to BO defects. Carrier lifetime was once again measured in the light-soaked state (τ_{LS}), with *NDD* then calculated as ($\tau_{LS}{}^{-1} - \tau_{DA}{}^{-1}$). This *NDD* is referred to as the initial *NDD* ($NDD_{initial}$), with measured carrier lifetimes referred to as $\tau_{DA,initial}$ and $\tau_{LS,initial}$ to distinguish them from later measurements.

All wafer groups were then fast-fired in a SierraTherm infrared belt furnace at varying peak firing temperatures (T_{peak}) at a belt speed of 200 in. per minute (roughly 5 m/min). In addition, wafers in Group A (SiN_x:H passivated samples) were fired one or more times ($N_{fire} = 1$, 2 or 3, where N_{fire} refers to the number of firing cycles). The temperature profile of firing profiles was determined using a Datapaq Q18 thermal profiler by measurements on dummy wafers prepared and fired identically to the samples in this study. The *NDD* was once again determined for all samples after firing (NDD_{fired}) using lifetime measurements following dark annealing ($\tau_{DA,fired}$) and light soaking ($\tau_{LS,fired}$) using the same procedure described earlier. Following this, some wafers were subjected to a 2-h illuminated annealing process (185 ± 2 °C, 0.80 ± 0.02 suns) to attempt to induce regeneration starting from the fully degraded state [7]. The carrier lifetime after regeneration (τ_{regen}) was then measured and the *NDD* after regeneration (NDD_{regen}) was calculated as ($\tau_{regen}{}^{-1} - \tau_{DA,fired}{}^{-1}$).

To better quantify the impact of firing and regeneration separately, it is necessary to determine the relative change in *NDD* before and after the process of interest. This relative change is further normalised via a quantity termed the fractional defect density (*FDD*) and is calculated separately for firing-induced changes (FDD_{firing}) and regeneration-induced changes (FDD_{regen}) as follows:

$$FDD_{firing} = 1 + \frac{NDD_{fired} - NDD_{initial}}{NDD_{initial}} = \frac{NDD_{fired}}{NDD_{initial}} \tag{1}$$

$$FDD_{regen} = 1 + \frac{NDD_{regen} - NDD_{fired}}{NDD_{fired}} = \frac{NDD_{regen}}{NDD_{fired}} \tag{2}$$

FDD so defined leads to a value of 1 when no change in *NDD* occurs after firing (or after regen), and leads to a value of 0 when firing (or regeneration) leads to total deactivation of the defect (i.e. when *NDD* after the process becomes zero).

Unless otherwise noted, all lifetime measurements in this study are reported at an injection level corresponding to $\Delta n = 0.1 \times N_A$, where Δn is the excess minority carrier density, and N_A is the base doping density (9.1×10^{15} cm^{-3} and 8.0×10^{15} cm^{-3} for the SiN_x:H- and SiO_2-passivated samples respectively).

3. Thermal deactivation and regeneration

This section presents the impact of surface preparation (i.e. hydrogen-rich SiN_x:H versus hydrogen-lean SiO_2) and firing conditions (peak temperature and multiple firing cycles) on the total number of BO defects. The results are discussed in the context of separate paths to permanently deactivate BO defects – a purely thermal process versus hydrogen passivation of the fully formed defect.

3.1. Deactivation during rapid firing

The impact of peak firing temperature on FDD_{firing} in Groups A (SiN_x:H passivated) and B (SiO_2 passivated) are plotted below in Fig. 1. All samples displayed similar $NDD_{initial}$ (i.e. before firing, not shown), whereas a large variation in NDD_{fired} was obtained after firing. This resulted in a reduction in FDD_{firing} for all samples and was strongly dependent on the firing conditions as seen in Fig. 1. FDD_{firing} decreased with increasing T_{peak} up to $T_{peak} = 632$ °C and then remained relatively constant up to $T_{peak} = 735$ °C. It can be seen that FDD_{firing} for both SiO_2 and SiN_x:H passivated samples follow almost identical trends with T_{peak}.

The trends in FDD_{firing} for $T_{peak} \leq 632$ °C largely agree with results from other studies, which also show a decrease in *NDD* with firing in this temperature range [11,13,27,28]. However, in some of the studies, *NDD* continues to decrease up to a set-point temperature, T_{set}, of 1050 °C before increasing again [10], whereas in others, *NDD* appears to increase with T_{set} for T_{set} higher than at least 650 °C [13]. Differences in the sample passivation and/or thermal ramp conditions could be responsible for lower *NDD* achieved after thermal treatments in such studies.

A slight rise in the level of FDD_{firing} was observed for samples fired at T_{peak} higher than 632 °C. This is attributed to the introduction of a small concentration of non-BO related CID-causing defects. Fitting of

Download English Version:

https://daneshyari.com/en/article/6456772

Download Persian Version:

https://daneshyari.com/article/6456772

Daneshyari.com